Antibiotic−Phospholipid Interactions as Studied by DSC and X-ray Diffraction

Cécile Grabielle-Madelmont,*,† Ambjörg Hochapfel,‡ and Michel Ollivon†

Equipe Physicochimie des Systèmes Polyphasés, UMR CNRS 8612, Université Paris-Sud, 92296 Châtenay-Malabry Cedex, France, and Groupe de Recherche en Physique et Biophysique, EA 228, Université René Descartes-Paris V, 45 rue des Saints Pères, 75270 Paris Cedex 06, France

Received: January 28, 1999; In Final Form: March 23, 1999

The interactions of the antibiotic lasalocid (LAS) as sodium salt with dipalmitoylphosphatidylcholine (DPPC) multilayers were analyzed in aqueous buffer (pH 7.4) for antibiotic/lipid molar ratios (r) ranging from 0 to 0.12. The study was performed both by X-ray diffraction as a function of temperature (XRDT) and by differential enthalpimetry (DSC). The effect of the antibiotic on the structural arrangement of the phospholipid bilayers is concentration dependent. For $0 \leq r \leq 0.04$: (i), the lamellar $L_{\beta'}$ phase of DPPC is progressively transformed into a new lamellar phase (called Lx) which displays a higher periodicity. Its composition corresponds to 1 mol of LAS per 25 mole of DPPC ($r = 0.04$); (ii) no significant structural changes are observed in the L_α phase. This finding is important for biological applications of the antibiotic; (iii) the thermotropic behavior is not markedly affected. Inversely, above $r = 0.04$, a strong perturbation of the DPPC acyl chain organization is observed which is accompanied by the formation of nonlamellar structures. The disappearance of a lamellar organization for $r = 0.08$ reflects the destructive effect of lasalocid on the lipidic membrane. The structural and thermal behavior may be explained by two localizations of the LAS molecules in the DPPC multilayers: at $r \leq 0.04$, the ionophore molecules as monomers lie parallel to the membrane surface and at $r > 0.04$, the ionophore as dimers insert in the DPPC bilayer perpendicular to the membrane surface. The change of the orientation of the antibiotic molecules occurs at a specific r corresponding to the composition of the Lx phase. A model for the distribution of the antibiotic molecules in the Lx phase is proposed. A schematic phase diagram is discussed.

Introduction

The mechanisms of antibiotic action are multiple. Many types of antibiotic molecules have been classified according to localization of their target within the cell. Whatever the type of antibiotic and its mode of action, transmembrane passage is an unavoidable preliminary step. Therefore, interaction of antibiotics with membrane molecules is of basic interest. The recent occurrence of multiresistance mechanisms from genetically selected bacteria, which jeopardize anti-infectious therapeutic treatments, enhances the need to understand the molecular process of antibiotic intake by the cells.

Among the different antibiotics, polyether ionophores possess the ability to bind and transport certain ions, and each antibiotic has its own specificity. For these reasons they are important biochemical tools in studying the role of cations in biological systems.[1] This class of ionophores is interesting as an example of mobile carriers because the molecule itself is involved in the ion transportation process across the membrane. Such ionophores possess (i) both polar and nonpolar groups, one next to the other, (ii) a stable conformation which directs the polar liganding moieties into a central cavity suitable for encaging a cation, and (iii) fast transport ability.[2] The carboxylic polyether ionophores are widely employed in biochemistry for analyzing the effect of transmembrane cation gradients on the function of cells and their organelles.[3]

Lasalocid is a carboxylic ionophore isolated from *Streptomyces lasaliensis* which forms complexes with most of the cations as well as some biogenic amines. These complexes exist in the solid state,[4−6] in solution,[7−9] and in mono- and bilayer membrane systems.[7,10−12] Many studies have been directed toward understanding the conformational dynamics of lasalocid A[2,3,13−15] and its cation complexes[8,9,15−18] in solution as well as the mechanisms of ionophore-mediated cation transport across membranes.[2,11,15,19−25]

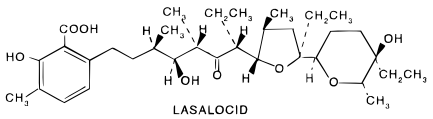

Because of the flexibility presented by the ionophore molecule, lasalocid conformation is very sensitive to the polarity of its environment. Highly polar solvents favor an acyclic conformation which progressively evolves to a cyclic one as the solvent polarity decreases.[2,15] The polarity-dependent conformers of lasalocid allow it to mediate ion transport across biological or model membranes. Lasalocid chelates the cation through ether, carbonyl, and hydroxyl oxygens resulting in a cyclic cation inclusion complex.[2,3] The currently proposed mechanism for cation transport across a membrane involves successive steps: the acyclic ionophore bound to the polar membrane interface by ion pairing to the terminal carboxylate moiety captures the cation. The complex rendered lipophilic by the hydrophobic backbone of the ionophore is able to diffuse across the apolar membrane interior to the opposite side. There,

* To whom correspondence should be addressed. E-mail: cecile.grabielle@cep.u-psud.fr. Fax: 33 (1) 46 83 53 12.
† Université Paris-Sud.
‡ Université René Descartes-Paris V.

10.1021/jp990340a CCC: $18.00
Published on Web 04/30/1999

the polar environment of the membrane interface restores the acyclic conformation of the ionophore with concomitant release of the cation.[9,15]

The intrinsic fluorescence of lasalocid A, which originates from its salicylic residue, has been used to obtain information about the degree of binding of the ionophore to phospholipidic membrane and its location in the membrane. Whatever the lipidic vesicles chosen as membrane models, monolayer dimyristoyl phosphatidylcholine (DMPC) vesicles (i.e., 50 nm diameter spheres of di-*n*-butyl ether covered with a monolayer of phospholipid molecules),[7,16] DPPC multilayer vesicles,[26] or small DMPC unilamellar vesicles,[27] fluorescence measurements indicate that lasalocid anion or at least its chromophore is located in the polar headgroup of the vesicle membrane at the aqueous interface. Localization of the ionophore in the polar headgroup has also been shown by circular dichroism spectroscopy[27] and ^{31}P NMR.[28] However, ^{1}H NMR line width measurements evidence that, for unilamellar vesicles, part of the ionophore molecules may penetrate the hydrophobic interior of the vesicles, which is not the case for multilamellar vesicles.[28] Interaction of the ionophore with phospholipid bilayers occurs as seen by changes in the thermotropic behavior of the pure phospholipid.[26,28,29]

Aggregation of lasalocid in membranes has been evidenced by monitoring the intrinsic fluorescence of this molecule. The existence of self-quenching of fluorescence above a certain amount of the ionophore results from association of lasalocid molecules in the membrane.[30] Measurements of the compression isotherms of lasalocid−Na salt inserted in DPPC monolayers indicate that the antibiotic molecules could also be aggregated in monolayers.[31,32]

Although direct interaction of lasalocid with membranes has been clearly evidenced, the implications of such interaction on the structural organization of the lipidic membrane have not been investigated. In this paper, modifications of the structural features of DPPC multilayers upon insertion of increasing concentration of lasalocid A sodium salt (LAS) were simultaneously examined by differential enthalpimetry (DSC) and X-ray diffraction measurements as a function of temperature (XRDT). Combination of both techniques is particularly convenient to correlate the structural changes to the thermotropic ones. The aim of this study is to obtain information on the effect of LAS on lipid bilayer packing, orientations of the lipid long-chain axes with respect to the bilayer normal, and the extent of insertion of the ionophore within the interior of the membrane. This study completes previous investigations on the implantation properties of lasalocid in monolayers[31−33] and multilayers[29] as model membranes. It also provides an interesting model for the interactions between two types of amphiphilic molecules, those for which the hydrophilic moiety is located at one extremity of a long hydrophobic chain (e.g., phospholipids) and those for which the polar/apolar character is laterally distributed along the molecule axis, as for lasalocid.

Experimental Section

Materials. 1,2-dipalmitoyl-*sn*-3-phosphatidylcholine (DPPC) (purity 99+% crystalline) was purchased from Sigma (St. Louis, MO) and used without further purification. The antibiotic lasalocid as sodium salt provided from Sigma was first recrystallized from aqueous methanol and then from a cyclohexane−acetone mixture. All of the samples were prepared in a 10 mM hepes (*N*-2-(hydroxyethyl)-2 piperazine *N*′-2-ethanesulfonic acid) (Sigma), 145mM NaCl (Prolabo, France) buffer (pH 7.4).

Sample Preparation. A stock solution of the antibiotic at a concentration of 2.5 10^{-3} M was prepared in chloroform. Lasalocid and DPPC at the required antibiotic/lipid molar ratio were first codissolved in chloroform/hexane (2:3 v/v). The solvents were distilled on molecular sieve for moisture removal. The solvent was removed under a nitrogen stream followed by drying under vacuum at 35 °C for 3 h. The dry film was then hydrated with buffer at 70 mM lipid concentration. The suspensions were vortexed twice for 3 min at 48 °C and then sonicated in a low-power sonifier (60 W) of bath type in order to promote the formation of multilamellar bilayers. These suspensions were used for both X-ray diffraction and DSC measurements.

X-ray Diffraction (XRDT). DPPC and LAS/DPPC suspensions were heated above the chain melting transition temperature of DPPC and vortexed in order to ensure good sample homogeneity. An aliquot (20 μL) of the samples was then loaded into a Lindemann glass capillary (external diameter = 1.35 ± 0.15 mm) with a wall thickness of 0.01 mm (GLAS, Müller, Berlin, Germany). Low-speed centrifugations (<1000 rpm) were used to concentrate the lipidic phase down to the bottom of the capillary. The capillary was filled with argon and closed by a drop of melted paraffin to prevent water evaporation. The suspensions separate into a lipidic rich phase and a clear water rich phase, thus demonstrating full hydration.

X-ray small angle diffraction measurements were carried out using a monochromatic (1.489 Å) focused X-ray beam at station D-24 of the DCI synchrotron at L.U.R.E. (Orsay, France). X-ray diffraction patterns were recorded using the initial setup of P. Vachette and C. Bourgaux. For all of the experiments, we used a sample holder specifically developed for the D24 station,[34] which allows X-ray diffraction patterns to be recorded as a function of temperature (XRDT). The temperature of the sample was measured by a thermocouple in contact with the sample capillary and recorded by a computer as a function of time. The temperature was linearly scanned, with an accuracy of 0.1 °C, with a temperature controller driven by a computer (EUROTHERM 902P). The intensities of the diffraction lines were recorded on a 1024 channel linear detector using an Ar/CO_2^- mixture as the gas stream. X-ray data were stored in a microvax computer through a specific acquisition bus (Camac) which allows to acquire up to 24 frames of the same duration (from 1 to 2000 sec) separated by a dead time of 1 s between frames.

X-ray measurements were performed by using the procedure defined for the study of the DPPC/octyl, β-D-glucopyranoside/water phase diagram.[35] Static experiments were done at 25 and 45 °C with an exposure time of 10 min. During the recordings as a function of temperature, 21 frames of 160 s were collected consecutively at 0.4 °C/min over a temperature range of 25−45 °C. For both types of experiments, two different sample-to-detector distances were used, 1420 and 283 mm, to explore two distinct regions of the X-ray diffraction pattern, one at low angles ($0 \le q \le 0.4$ Å^{-1}) and the other at wide angles ($0 \le q \le 2$ Å^{-1}). The parameter $q = 4\pi \sin\theta/\lambda$, where 2θ is the scattering angle and λ the wavelength, defines the positions in the reciprocal space.

The diffraction patterns were normalized with respect to synchroton beam decay and acquisition times using a homemade software program. The diffraction spacing was calibrated by using highly purified tristearine with a repeat distance of 45 Å.[36] The Bragg spacings (d(Å) = $n\lambda/2\sin\theta$, with n = an integer) were calculated from the maximum of the diffraction peaks

determined by fitting the curves. For each sample studied, the plot of the repeat distance versus temperature displays break points corresponding to phase transitions. The transition temperatures were taken at the onset of the transition and were determined from the intersection of the straight lines obtained by linear regression analysis of the spacing values measured on either side of the transition.

Differential Scanning Calorimetry (DSC). DPPC and LAS/DPPC suspensions (150−200 mg) homogenized as above were transferred to stainless steel sample holders. The experiments were carried out using a high sensitivity ARION microcalorimeter of flux type (sensitivity 100 μV/mW at 40 °C). The advantages of such a calorimeter are (i) a large sample size allows for accurate definition of composition and favors detection of weak thermal effects, (ii) the use of a very low heating rate (0.08 °C/min) favors peak resolution and sample temperature homogeneity and ensures a better equilibrium state as a function of temperature, and (iii) the sample can be recovered after analysis.

The samples were analyzed at a heating rate of 0.08 °C/min in the temperature range of 5−45 °C. The water content was controlled by weighing before and after each calorimetric recording. Highly purified lauric acid was used to standardize the apparatus for temperature and quantitative heat determination. The transition temperatures were taken at the onset of the transitions, i.e., at the intercept of the tangent to the low-temperature side of the thermal peak with the baseline.[37] The transition enthalpy changes (ΔH) were determined from the peak areas by weighing. Repeated heating scans gave reproducible results. The thermal behavior of the LAS/DPPC mixtures versus time is very stable, as previously demonstrated.[29]

Results

Eleven LAS/DPPC mixtures corresponding to molar LAS/DPPC ratios (r = 0.0, 0.005, 0.01, 0.02, 0.03, 0.04, 0.05, 0.06, 0.08, 0.1, 0.12) have been studied as a function of temperature from 25 to 45 °C by both DSC and XRDT at constant DPPC concentration (70 mM) corresponding to fully hydrated conditions.

X-ray Measurements. The X-ray diffraction patterns were recorded both at wide angles to get information about the packing of the phospholipid hydrocarbon chains (spacings around 4 Å; $1.2 \leq q \leq 1.7$ Å^{-1}) and at low angles to obtain the long-range organization of the lipid assemblies (spacings from 200 to 20 Å; $0.02 \leq q \leq 0.40$ Å^{-1}).

Wide-Angle Diffraction. The wide-angle pattern of DPPC at 25 °C displays a sharp reflection at 4.2 Å with a shoulder located at 4.1 Å in relation to the disordered orthorhombic hybrid lattice characteristic of the gel phase $L_{\beta'}$.[38−40] This wide-angle double reflection is also detected for DPPC multilayers containing LAS up to r = 0.02 (Figure 1A). For $r > 0.02$, only the sharp reflection at 4.2 Å is observed and the peak profile becomes symmetrical, indicating a hexagonal chain packing.[38] At 45 °C, all of the suspensions, whatever the amount of LAS, give a diffuse reflection centered at 4.6 Å corresponding to melted chain states (Figure 1B).

The wide-angle diffraction patterns observed for the different LAS/DPPC ratios present a similar behavior as a function of temperature. They all show the existence of a transition from an ordered to a disordered chain packing which indicates that a DPPC hydrocarbon chain organization still persists at r = 0.12. The evolution corresponding to pure DPPC and a high LAS/DPPC ratio (r = 0.08) is given in Figure 2 for illustration.

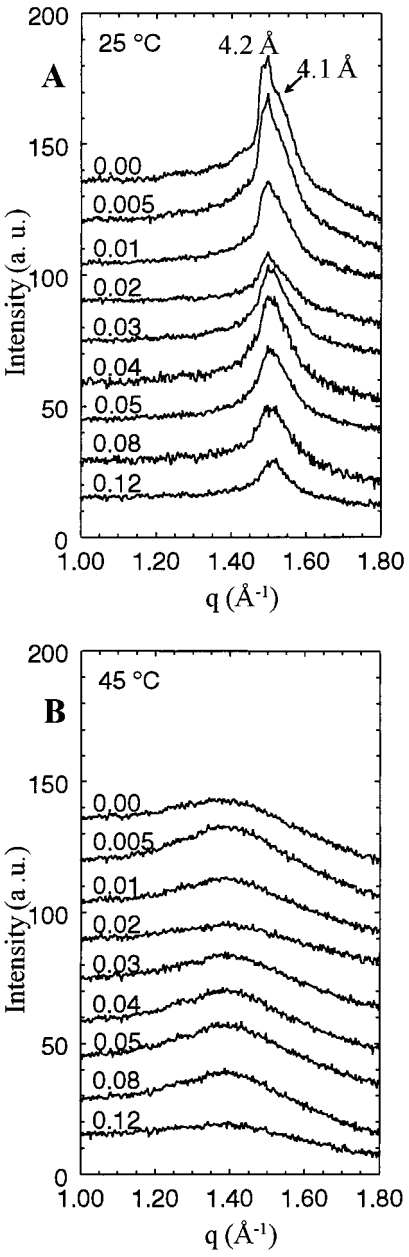

Figure 1. Wide-angle X-ray diffraction patterns of LAS/DPPC mixtures versus LAS/DPPC molar ratio (r) at (A) 25 °C and (B) 45 °C.

Low-angle Diffraction Data. Evolution of the Long Spacings as a Function of r at 25 °C. X-ray diffraction patterns recorded at 25 °C from fully hydrated DPPC samples containing an increasing amount of LAS ($0 \leq r \leq 0.12$) are shown in Figure 3A, and the corresponding long spacings reported in Table 1. The sharp lamellar reflections (n = 1−4) recorded for pure DPPC are also observed in the presence of the antibiotic up to r = 0.01. However, the insertion of LAS in DPPC multilayers even at r = 0.005 slightly broadens the width of the DPPC lamellar reflections (Table 1). For r = 0.01, a shoulder centered in the lower q region is clearly observed both on the first- and the second-order reflections. At r = 0.02, the amplitude of this new lamellar reflection is amplified whereas that related to pure DPPC decreases. For $0.03 \leq r \leq 0.06$, the lamellar reflections of pure DPPC no longer exist and only these new lamellar reflections are recorded. This indicates the occurrence of a new lamellar structure (called Lx in the discussion section) which coexists with that of pure DPPC for r = 0.01 and r = 0.02. For

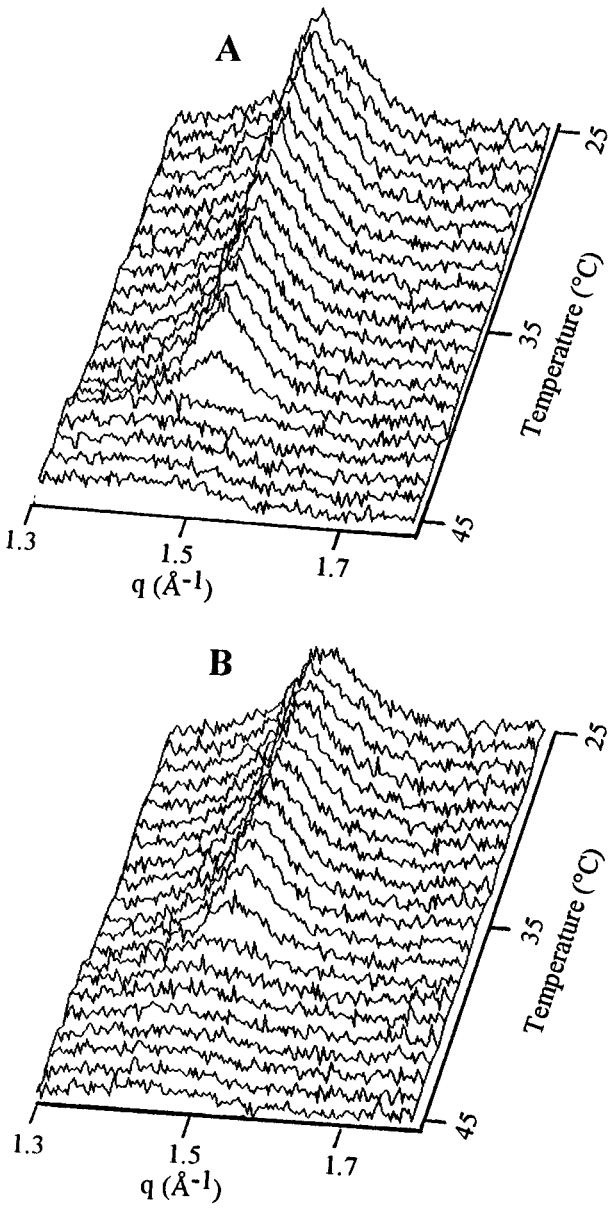

Figure 2. Typical evolution of the wide-angle X-ray diffraction patterns as a function of temperature for (A) pure DPPC and (B) LAS/DPPC molar ratio $r = 0.08$.

$r > 0.06$, two broad diffraction peaks (Figure 3A) are recorded indicating at least a strong deviation from a regular lamellar organization because $d_{001} \neq d_{002} \times 2$ (Table 1).

Evolution of the Long Spacings as a Function of Temperature. For each antibiotic:lipid ratio studied, the diffraction patterns recorded from 25 to 45 °C at a heating rate of 0.4 °C/min, are reported as a function of temperature in Figure 4. Bragg spacings and half-height widths of the diffraction peaks at selected temperature are summarized in Table 1 and XRDT transition temperatures determined as described in the experimental section are reported in Table 2.

$0 \leq r \leq 0.04$. With increasing temperature, the lamellar reflections characteristic of the gel $L_{\beta'}$, the rippled $P_{\beta'}$, and the liquid-crystalline L_α phases of DPPC (Figure 4A, Table 1**)** are clearly observed up to $r = 0.02$ (Figure 4B−D). For $r = 0.005$, the diffraction pattern remains very similar to that of pure DPPC. However, the lamellar reflection relative to the DPPC $L_{\beta'}$ structure is widened between 25 and 30 °C (Figure 5A) toward the lower q region where the presence of a new lamellar phase is clearly detected from $r = 0.01$. For $r = 0.01$, the new phase

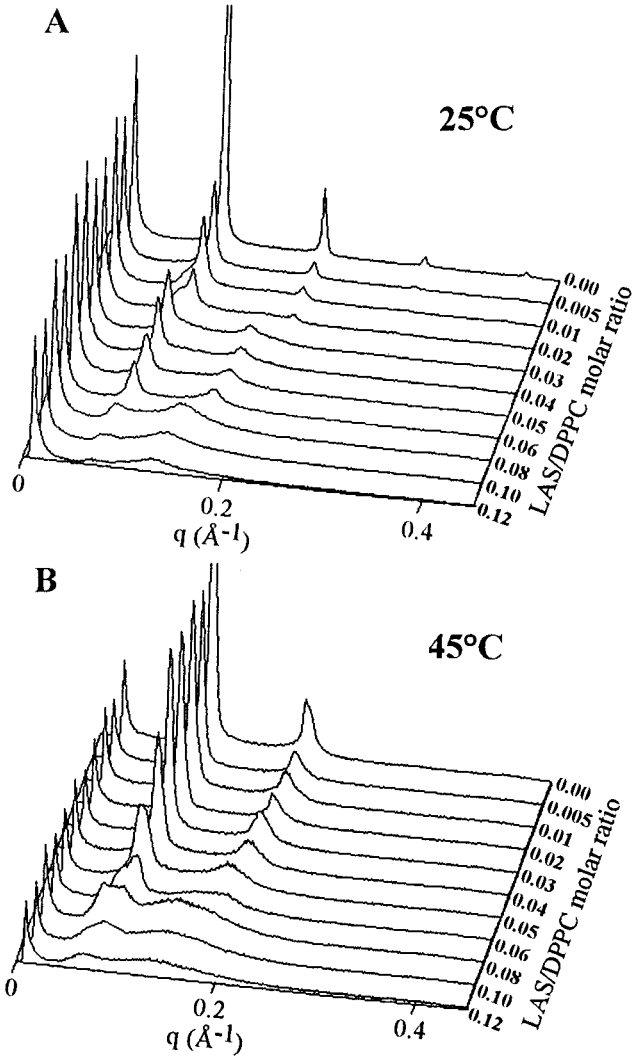

Figure 3. Low-angle X-ray diffraction patterns of LAS/DPPC mixtures versus LAS/DPPC molar ratio (r) at (A) 25 °C and (B) 45 °C.

which appears at 25 °C as a shoulder centered around 70.7 Å on the DPPC $L_{\beta'}$ diffraction peak (bilayer periodicity 63.8 Å) gives progressive rise to a distinct diffraction peak when the temperature increases (Figure 5B). The relative amplitude of both diffraction peaks is temperature dependent. The same behavior is observed for $r = 0.02$, except that the amplitude of the shoulder (≈73.7 Å) is more pronounced, indicating that the proportion of the new phase in coexistence with the DPPC $L_{\beta'}$ phase becomes more important (Figure 5C). Above 34 °C, globally only the reflections relative to the DPPC $P_{\beta'}$ structure are depicted in the 0.005−0.02 molar ratio range (Figure 4A−D, Table 1), whereas the temperature at which this phase appears decreases with increasing r (Table 2). This structure, which consists of lipid lamellae distorted by a periodic undulation,[38,41,42] is characterized by a main diffraction peak corresponding to a periodicity higher than that of the $L_{\beta'}$ phase, associated with a shoulder on the high q side of the reflection. This phase is also characterized by a very small reflection located at a low q which has been attributed to the ripple repeat distance (140 Å) (Figure 6). This weak reflection exists over the temperature range of the DPPC $P_{\beta'}$ phase and disappears at the $P_{\beta'} \leftrightarrow L_\alpha$ transition.[38,42] In the low-angle diffraction patterns, this weak reflection is recorded up to $r = 0.02$ between 35 and 39 °C whereas it is no longer detected for $r = 0.04$ (Figure 6). This indicates that a number of DPPC molecules still adopt the ripple organization of the $P_{\beta'}$ phase of DPPC in the LAS/DPPC

TABLE 1: Bragg Long Spacings and Half-Height Widths of the Diffraction Peaks as a Function of the Antibiotic/DPPC Molar Ratio (*r*) for Three Selected Temperatures[a]

	25 °C			36 °C			45 °C		
r	d_{001} (Å)	$d_{002} \times 2$ (Å)	half-height width $q \times 10^3$ (Å^{-1})	d_{001} (Å)	$d_{002} \times 2$ (Å)	half-height width $q \times 10^3$ (Å^{-1})	d_{001} (Å)	$d_{002} \times 2$ (Å)	half-height width $q \times 10^3$ (Å^{-1})
0	63.7	63.3	3.45	72.5 + sh	69.5 + sh	9.21	66.4	66.5	6.14
0.005	63.8	63.2	6.14	71.5 + sh	71.0 + sh		66.7	66.5	6.14
0.01	sh + 63.8	sh + 63.3		72.5 + sh	70.0 + sh		66.6	66.7	7.48
0.02	sh + 64.1	sh + 63.6		73.6 + sh	72.7 + sh		67.6	67.4	6.14
0.03	75.8	75.9	8.25	74.7 + sh	74.9 + sh		69.0	68.8	7.67
0.04	75.7	75.7	8.05	74.8	74.9	6.71	69.5	69.3	10.74
0.05	77.0	77.0	11.51	77.1	76.9	6.90	sh + 73.9	73.6	
0.06	79.2	79.3	10.36	79.3	78.9	5.18	86.9/70.7	83.4/71.9	
0.08	86.0	91.2		87.2	87.0	11.51	93.1/74.2	90.0/72.5	
0.10	85.3	96.0		90.5	93.1		81.8	91.6	
0.12	92.9	98.2		89.9	92.2		93.8	94.4	

[a] The half-height width of the diffraction peaks was determined only when the peaks presented no shoulder (sh = shoulder).

TABLE 2: Evolution of the Thermodynamic Data Determined by DSC (*T*, °C; ΔH, kJ mol^{-1} of DPPC) and XRDT (*T*, °C) as a Function of LAS/DPPC Molar Ratio (*r*)[a]

	DSC				XRDT		
					short spacings	long spacings	
r	T_{pre} (°C)	T_1 (°C)	T_{main} (°C)	T_2 (°C)	T_{main} (°C)	T_{pre} (°C)	T_{main} (°C)
0	35.21		41.46 (34.9)		41.3	33.8	40.1
0.005	33.47		40.96 (34.2)		41.4	32.8	39.8
0.01	33.46		40.98 (35.4)		41.1	31.1	40.1
0.02			40.74 (36.2)		41.0	29.3	39.8
0.03			40.75 (36.5)		40.3		38.9
0.04			40.13 (33.4)		40.3		38.24
0.05			39.19 (32.8)[b]		40.1		38.9
0.06		38.59	39.26 (37.6)[b]	40.89			37.7
0.08		38.59		41.23	38.7		34.9
0.10		37.05		40.03			35.0
0.12		35.89		40.02			35.0

[a] ΔH expressed as kJ mol^{-1} of DPPC are reported in parentheses. [b] ΔH of the whole transition. The temperatures correspond to the onset of the transitions (see the experimental section).

mixtures, but for $r = 0.04$ the undulation along the bilayer lamellae is removed. Besides, the main diffraction peak relative to the $P_{\beta'}$ phase stands nearly at the same q as the reflection associated with the new phase (Figure 6). For $r = 0.03$ only traces of the $P_{\beta'}$ phase are still visible (Figure 4E). For $r = 0.04$, the lamellar reflections ($d_{001} = d_{002} = 75.7$ Å) (Table 1) given at 25 °C by the new phase are continuously recorded up to 40 °C (Figure 4F). The peak position (taken at the baseline) is constant over this whole temperature range while its maximum (periodicity: 75.7 Å between 25 and 30 °C) is slightly shifted to the high q region between 30 and 38 °C (periodicity: 74.4 Å), leading to a decrease of 1.3 Å in the repeat distance as a consequence of a change in the symmetry of the peak. As well, a decrease of 1 Å is observed in the periodicity of the $P_{\beta'}$ phase of DPPC versus temperature (73.4 and 72.4 Å at 35 and 38 °C, respectively). It results that the characteristics of the lamellar Lx structure formed at 25 °C remain unchanged up to 40 °C so that it may be considered that the $P_{\beta'}$ phase of DPPC no longer exists (Figure 7A, B).

For $0 \leq r \leq 0.04$, the transition into the L_α phase occurs at a temperature close to that of pure DPPC (Table 2) leading to the formation of a single lamellar structure ($n = 2$) (Figure 4A–F) in which the hydrocarbon chains adopt a fluid state (Figures 1 and 2). At 45 °C, for $0 \leq r \leq 0.04$ the long spacing of this L_α phase slightly increases with r (Figure 3B, Table 1). This evidences that in the L_α phase LAS is still interacting with the DPPC membrane.

$0.05 \leq r \leq 0.12$. For $r = 0.05$ and 0.06, lamellar reflections are still observed between 25 and 37 °C (Figure 4G, H) with a repeat distance dependent on r ($d = 77$ and 79.2 Å for $r = 0.05$ and 0.06, respectively) (Figure 8A, Table 1) and independent of the temperature. The diffraction peaks observed are broader than the reflections corresponding to $r = 0.04$ (Table 1). This might be due to the existence of flatness defects of the polar headgroups surface as a consequence of the insertion of LAS. However, the diffraction peaks become sharper between 32 and 37 °C ($r = 0.05$) and 32 and 36 °C ($r = 0.06$), respectively (Figure 4G, H). For $r = 0.08$, the reflections deviate from a lamellar organization ($d_{001} \neq d_{002}$) at 25 °C (Table 1) and the second reflection is more intense than the first one (Figure 4I). The repeat distance (86 Å at 25 °C) is nearly constant up to 30 °C and then progressively increases up to 89

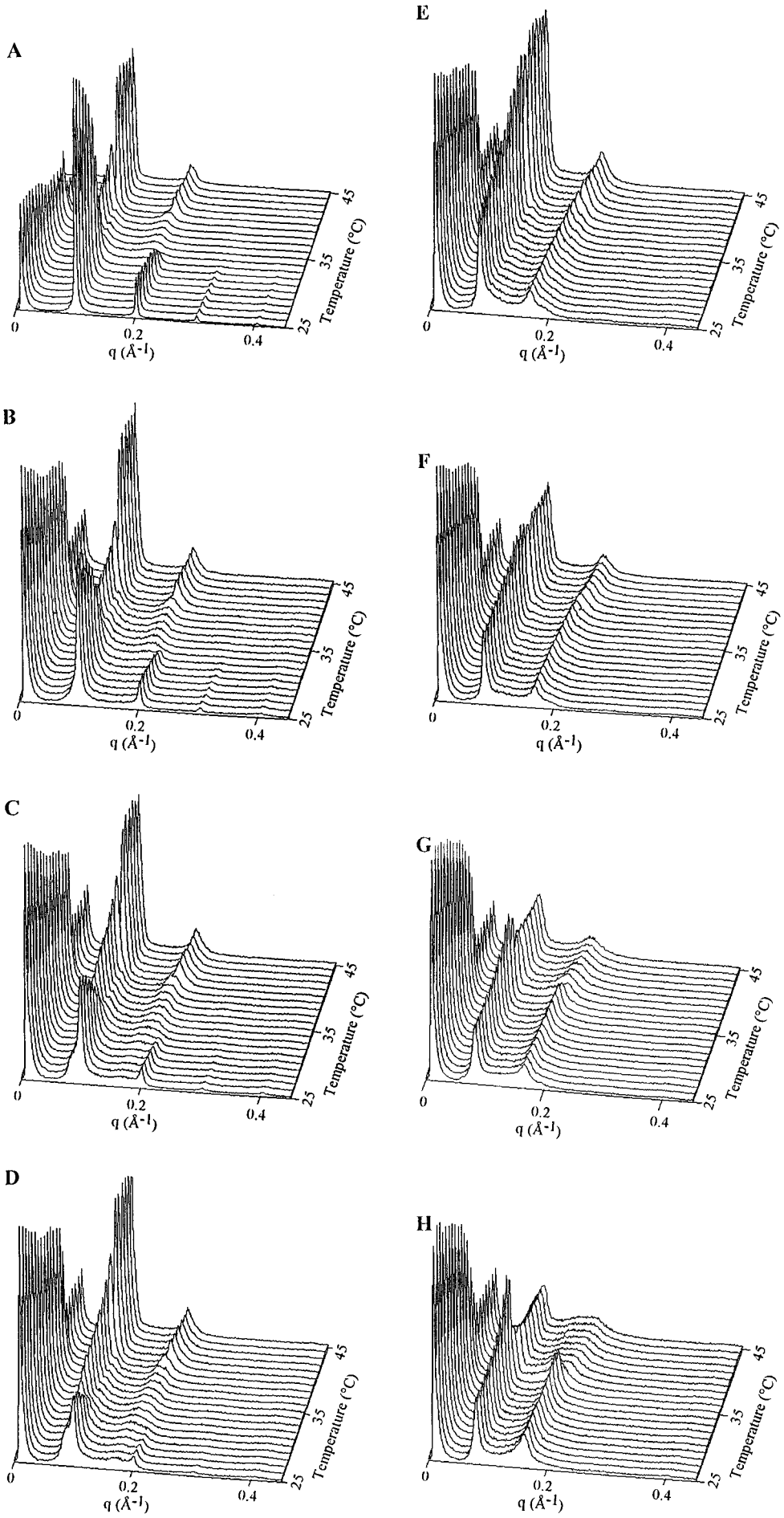
A
B
C
D
E
F
G
H
0
0.2
0.4
q (Å-1)
25
35
45
Temperature (°C)

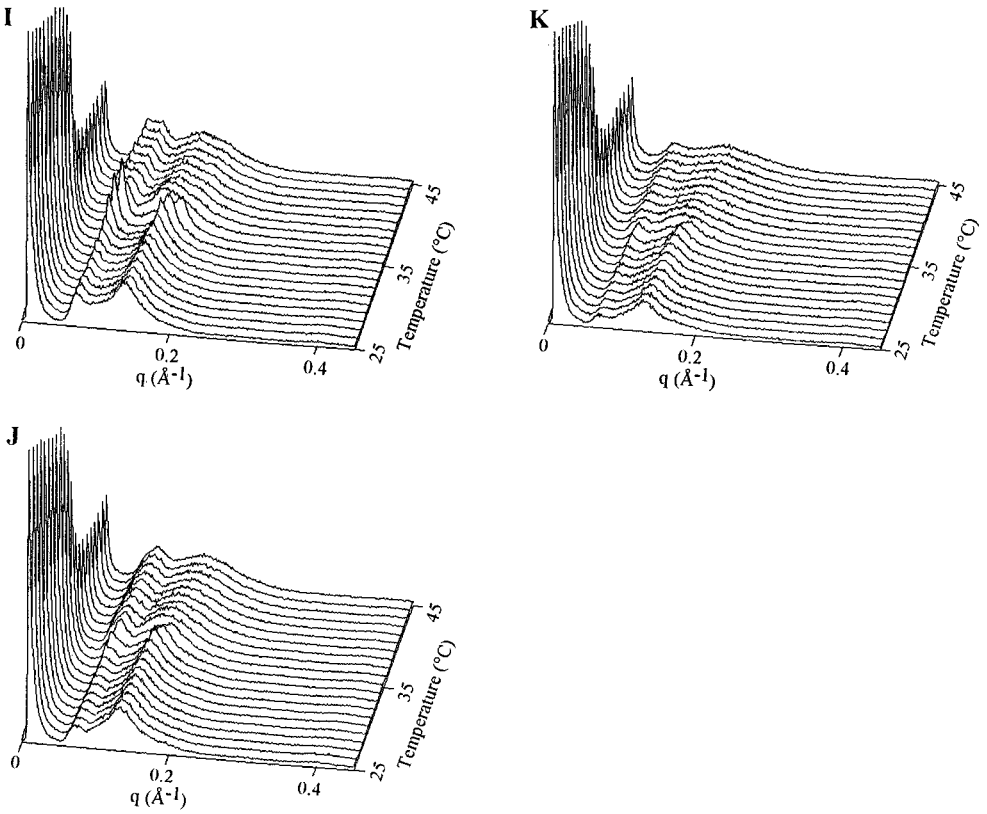

Figure 4. Evolution of the low-angle X-ray diffraction patterns of DPPC and LAS/DPPC mixtures as a function of temperature and ratio: (A) DPPC, (B to K) $r = 0.005$, 0.01, 0.02, 0.03, 0.04, 0.05, 0.06, 0.08, 0.1, and 0.12, respectively.

Å at 35 °C (Figure 8A). From 35 to 37 °C, whereas the diffraction peaks become sharper, the periodicity decreases from 89 to 80.6 Å and the two peaks recorded correspond again to the first and second order of a lamellar structure. This indicates that at least part of the lipidic membrane tends to adopt again a lamellar arrangement in this narrow temperature range.

Above 36−37 °C, a phase transition associated with drastic changes in the diffraction patterns is detected. Two double broad diffraction bands replace the two sharp reflections previously observed. In fact, this splitting is initiated from $r = 0.05$ and becomes more and more pronounced for $r = 0.06$ and 0.08 (Figure 8B). For $r = 0.05$, each double broad band is progressively transformed into a single one when the temperature reaches 44 °C, whereas for $r = 0.06$, the double band still persists at 45 °C. Above the transition, the repeat distances (Table 1) calculated from the double reflection indicate that one is higher and the other lower than the long spacing corresponding to the single reflection observed just below the phase transition. These results may be interpreted as the formation of two kinds of antibiotic/DPPC structural organization throughout the transition. By comparing the amplitude of these two broad reflections, the one with the higher periodicity is amplified when r increases. This could indicate that this organization becomes more preponderant.

For $r = 0.10$ (Figure 4J) and 0.12 (Figure 4K), the diffraction patterns exhibit two broad bands which may depict very disordered periodic structures. The more intense broad band (Figure 9A) corresponds to an apparent repeat distance centered at 48−49 Å (Figure 9B). On the low-angle side of this broad band, a peak of weaker intensity is observed. Whereas the long spacing relative to the second reflection does not change, the value associated with the first one increases with r and also with the temperature between 30 and 35 °C. An increase in the amplitude of the second reflection is also observed around 35 °C. A phase transition still occurs as demonstrated by the modification of the low-angle peak shape at 37 °C and the change of the short spacing from 4.2 to 4.6 Å (Figure 1). The general behavior strongly deviates from a lamellar organization even if the reflections get closer to a lamellar periodicity at 35−36 °C (Figure 9B). Thus, the ionophore progressively disrupts the lamellar organization of the DPPC membrane.

DSC Measurements. The calorimetric curves of pure and LAS incorporated DPPC multilayers at different ionophore/lipid ratios studied are shown in Figure 10. The thermodynamic data (transition temperatures and enthalpy change (ΔH) expressed as kJ mol^{-1} of DPPC) are gathered in Table 2 together with the transition temperatures given by X-ray diffraction measurements.

The pretransition and the main chain melting transition of pure DPPC are observed at 35.21 and 41.46 °C (Table 2), in agreement with the literature data.[37,43−46] In the low LAS concentration range ($r = 0.005$, 0.01, 0.02), a broadening of the pretransition with reduction in enthalpy is observed. The pretransition disappears at a LAS/DPPC ratio of 0.02. The main transition does not show any significant change. However, the thermal profiles present a slight broadening even if the ΔH is not affected. This indicates a slight decrease in the cooperativity of the chain melting transition. For $0.02 \leq r \leq 0.04$, the broadening of the main transition increases whereas its amplitude decreases. From $r = 0.05$, the DPPC main transition profile is significantly affected by the presence of lasalocid. Shoulders appear below and above the main peak. They become more pronounced for $r = 0.06$ and 0.08. For $r = 0.1$ and 0.12, the main peak is no more recorded while the previous shoulders give rise to distinct transitions. For $r = 0.05$ and 0.06, the total enthalpy change has been still expressed as kJ mol^{-1} of DPPC because the major part of the peak may be attributed to the lamellar structure relative to $r = 0.04$. The total enthalpy values

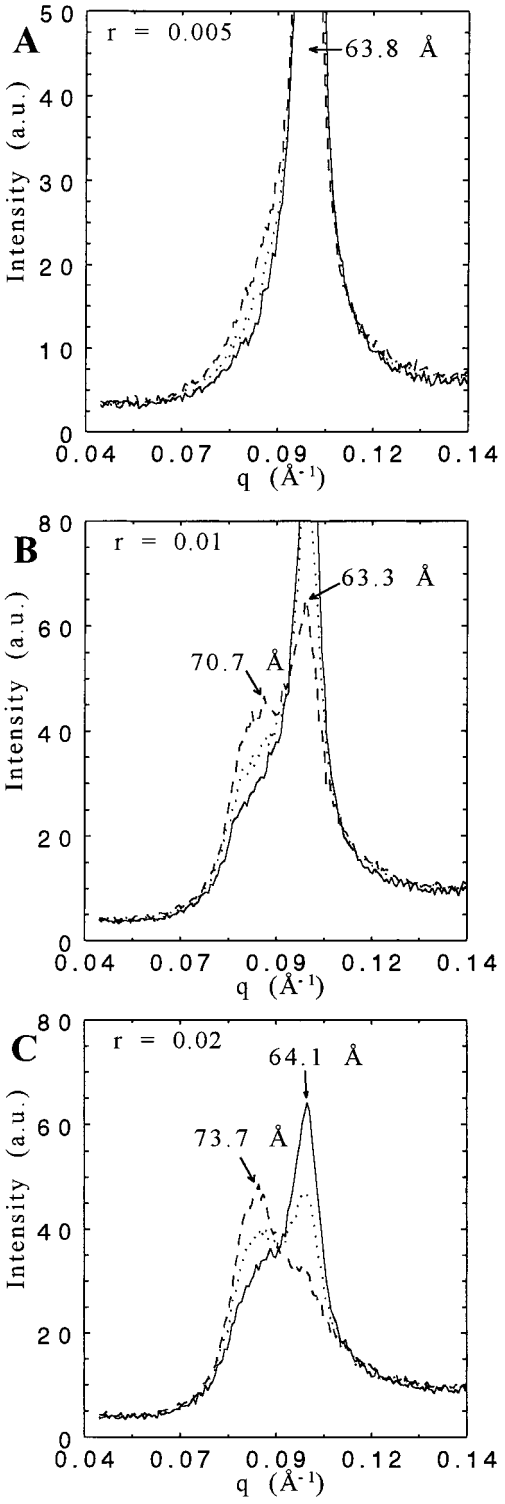

Figure 5. Coexistence of the lamellar LAS/DPPC Lx phase with the $L_{\beta'}$ phase of DPPC versus temperature as observed by low-angle X-ray diffraction: (—) 25 °C, (• • •) 28.5 °C, (- - -) 30.6 °C for (A) $r = 0.005$, (B) $r = 0.01$, (C) $r = 0.02$, respectively.

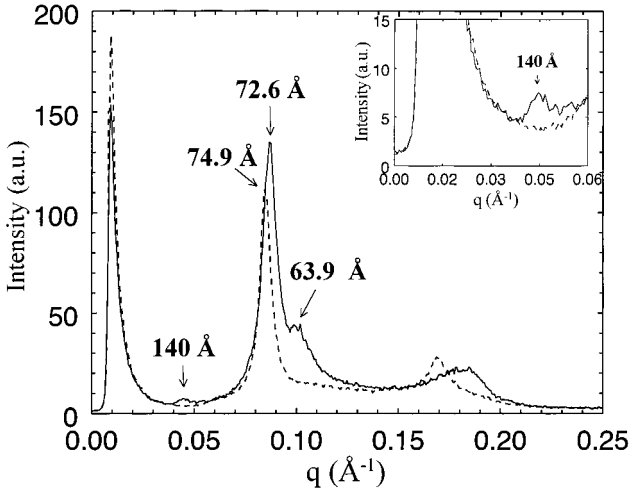

Figure 6. Low-angle X-ray diffraction patterns at 37 °C of the $P_{\beta'}$ phase of DPPC (—) and the Lx phase at $r = 0.04$ (- - -). Inset: enlargment of the $0 \leq q \leq 0.06$ Å^{-1} domain.

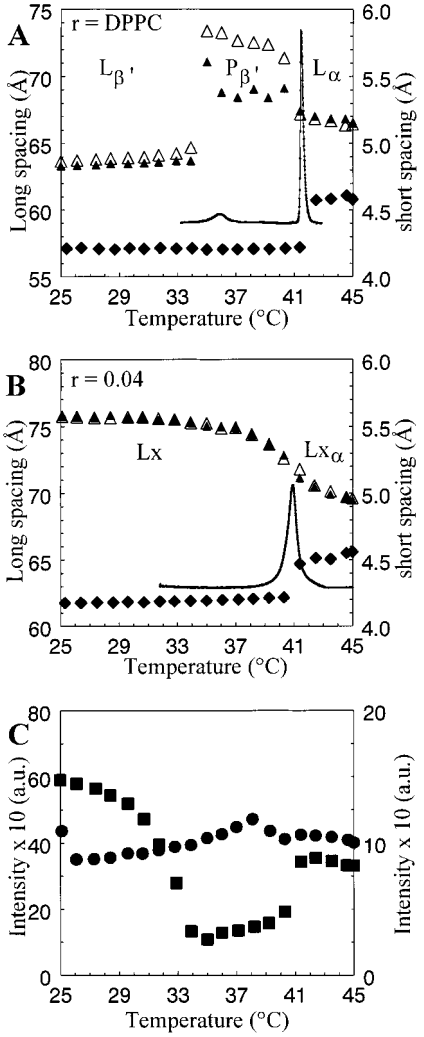

Figure 7. Thermal and structural behavior of (A) DPPC and (B) LAS/DPPC ratio $r = 0.04$ versus temperature: (—) calorimetric curve, (△, ▲) d_{001} and $d_{002} \times 2$ long and (◆) short spacings. (C) Evolution of the intensity at the maximum diffraction peak versus temperature for (■) DPPC and (●) $r = 0.04$.

obtained for the whole transition remain relatively similar to those found for the lower ratios. Beyond $r = 0.06$, the overlapped peaks do not allow to determine the actual ΔH relative to each transition.

Discussion

Interaction of LAS with phospholipidic multilayers is evidenced, even at very low r ($r \leq 0.01$), from the modifications observed in both the structural organization and thermal behavior of DPPC upon addition of the ionophore. The question addressed here is how XRDT and DSC may contribute to the understand-

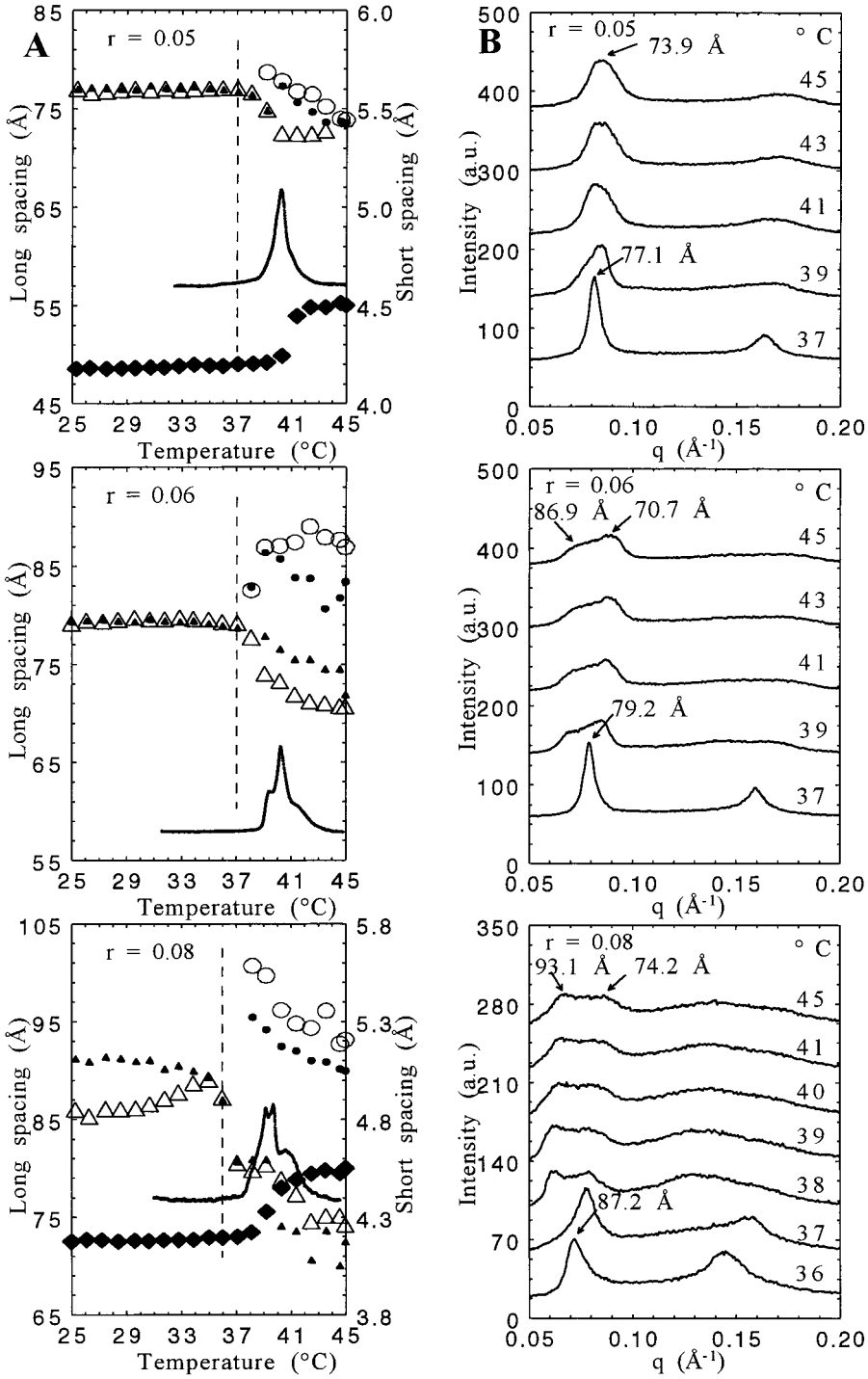

Figure 8. Thermal and structural behavior versus temperature for LAS/DPPC ratios $r = 0.05$, 0.06, and 0.08, respectively: (A) (—) calorimetric curve, (△, ○) d_{001} long spacing below and above 36 °C, respectively, (▲, ●) $d_{002} \times 2$ long spacing below and above 36 °C, respectively, and (◆) short spacings. The vertical dashed line delimits the temperature domain shown in (B). (B) Evolution of the low-angle X-ray diffraction patterns at selected temperature above 36 °C.

ing of the ionophore localization in the membrane and its consequence on the lipid structural arrangement.

In the LAS/DPPC mixtures, although the exact concentration of the ionophore in the membrane is not known, it can be reasonably assumed that no significant amount of lasalocid partitions into the aqueous phase, given the low aqueous solubility of LAS ($\approx 2\ 10^{-4}$ mol^{-1}.dm^{-3}),[18] its preferential affinity for lipid environment,[26,30] and the large excess of DPPC (70 mM) used in the LAS/DPPC molar ratios studied.

Both XRDT and DSC provide information about the structural evolution of the different mixtures examined as a function of temperature. Whatever the r values, there is an excellent agreement between the transition temperatures determined by the two techniques (Table 2). Therefore, both series of data can be compared through this parameter.

Structural Behavior of the LAS/ DPPC Multilayers. In excess of water, the DPPC multilayers (Figure 7A) display the well-known thermotropism.[38,39,47] Two liquid crystalline phases $L_{\beta'}$ and $P_{\beta'}$ with ordered chains, currently named "gel" phases, exist below the chain-melting transition, while a melted chain liquid crystalline phase L_α is observed above. A highly chain-ordered phase L_c may be obtained after a few days of storage

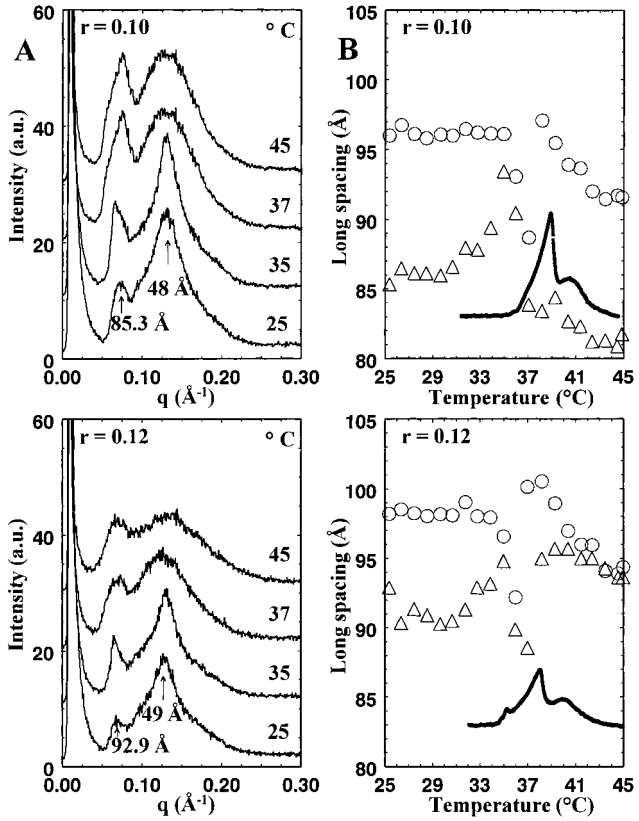

Figure 9. Thermal and structural behavior versus temperature for LAS/DPPC ratios $r = 0.10$ and 0.12, respectively: (A) Evolution of the low-angle X-ray diffraction patterns at selected temperatures. (B) (—) calorimetric curve, (△, ○) first and second × 2 reflections, respectively.

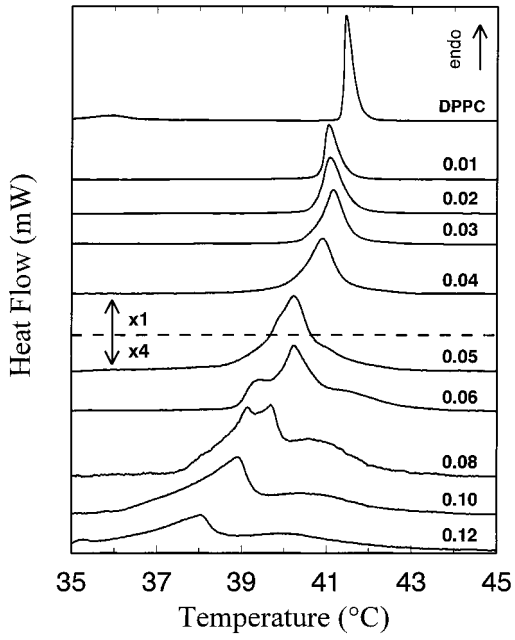

Figure 10. DSC recordings of LAS/DPPC mixtures. The samples (150 to 200 mg) were analyzed at a heating rate of 0.08 °C/min. The curves, normalized by weight, are plotted with two different *Y* scales (×1 and ×4). The signal/noise of the curve recorded for $r = 0.08$ is due to the small amount of the sample.

at low temperature.[39,48,49] This variety cannot be formed under the experimental conditions used in this study. Many low-angle diffraction studies have provided measurements of the lamellar repeat distances characteristic of the DPPC phases. They span a range from 63.5 to 64.2, 66 to 72.3, and 60 to 67.5 Å for the $L_{\beta'}$, $P_{\beta'}$, and Lα phases, respectively.[38−40,42,49−54] The values found in the present study (Table 1) are very close to those given in refs 40, 50, 52−54.

At 25 °C, for LAS/DPPC molar ratios ranging from 0.005 to 0.03, the L_{β}' phase of pure DPPC coexists with another lamellar phase (named Lx) of higher periodicity. As soon as some LAS molecules are added, changes in the lamellar organization of the DPPC bilayers occur as seen by the broadening of the low-angle reflection relative to the L_{β}' phase of DPPC observed for $r = 0.005$ between 25 and 35 °C (Figure 5A). These structural modifications may correspond to the very beginning of the phase separation between the DPPC $L_{\beta'}$ and the mixed LAS/DPPC Lx phases. The respective evolution of the peak intensities relative to the DPPC $L_{\beta'}$ and the Lx phases indicates that in the 0−0.04 molar ratio and 25−35 °C temperature ranges, the DPPC $L_{\beta'}$ phase is progressively replaced by the Lx phase (Figure 5).

For $r = 0.04$, the Lx phase exists as a single one (Figure 3A and 7B). Therefore, one molecule of LAS per 25 molecules of DPPC induces a unique lamellar phase, the repeat distance of which is larger than that of the L_{β}' phase of DPPC at 25 °C (Table 1). The symmetrical reflection corresponding to an interchain spacing of 4.2 Å (Figure 1) indicates that the interaction of LAS with DPPC modifies the lateral hydrocarbon chain packing of the membrane. This packing change, which corresponds to the transformation of the two-dimensional rectangular lattice of the L_{β}' phase of DPPC into a one-dimensional hexagonal lattice, evidenced by the fact that the peak profile becomes symmetrical, suggests a change in the orientational direction of the chains with respect to the bilayer normal.[38,47,55] The increase in the bilayer thickness observed in the Lx phase may result primarily from a loss of chain tilt and also from a change in headgroup conformation. Interaction of the antibiotic with the DPPC choline group may cause the choline group to adopt a more extended position, whereas in the $L_{\beta'}$ phase of DPPC, the hydrocarbon chains are tilted because the headgroup, oriented approximately parallel to the plane of the bilayer plane, occupies a larger area than the hydrocarbon chains.[56] At 25 °C, the repeat distance of the Lx phase (75.7 Å) is also close to the long spacing of the $P_{\beta'}$ phase of DPPC (72.5 Å) observed above 35 °C (Table 1). The formation of the $P_{\beta'}$ phase is associated with orientational changes in both the head polar groups and long-chain axis.[38,57−59] According to different authors, the hydrocarbon chains either present a reduced tilt[38,39,49] or become perpendicular[41,57] to the bilayer plane at the pretransition. The extent of the long spacing increase and the removal of the pretransition may provide evidence that the DPPC chains are oriented normal to the bilayer plane when the antibiotic is added. It is worth noting that pretransitions do not occur in bilayers with chains perpendicular to the bilayer plane.[56] Thus, at 25 °C, the two lamellar structures in coexistence would differ in the polar headgroup orientation and chain packing, i.e., the L_{β}' phase of DPPC with tilted chains and the Lx phase with chains normal to the plane of the lamellae. The formation of a homogeneous phase for $r = 0.04$ suggests that one molecule of the ionophore may change the orientation of 25 phospholipid molecules.

Between 35 and 40 °C, the $P_{\beta'}$ structure relative to the DPPC molecules unperturbated by LAS coexists with the Lx phase in the 0−0.04 molar ratio range. These coexisting phases present similarities regarding both the long- (72.5 and 74.8 Å at 36 °C for the $P_{\beta'}$ phase of DPPC and Lx phase, respectively) and short (4.2 Å) spacings (Figure 7A, B). The difference in the structural organization of these two phases lies in the fact that the $P_{\beta'}$ phase undergoes a ripple undulation along the plane of the

bilayers, whereas the LAS molecules interacting with the DPPC molecules in the Lx phase would impede the formation of the undulation as shown by the absence of the weak reflection centered at $q = 0.045$ Å^{-1} (Figure 6) and attributed to the ripple periodicity (140 Å).[38,41,42]

The molecular organization of the $L_{\beta'}$ phase of pure DPPC presents fluctuations with increasing temperature. Indeed, the continuous decrease in the amplitude of the diffraction reflections with increasing temperature (Figure 7C) suggests that the molecular arrangement of the $L_{\beta'}$ phase becomes disordered. Inversely, the amplitude and the profile of the reflections obtained for the new phase remain nearly unchanged over the whole temperature range of its existence (Figure 7C). At 25 °C, comparison of the half-height widths (Table 1) of the lamellar reflections detected respectively for the $L_{\beta'}$ phase and the mixed LAS/DPPC Lx phase indicates that this latter phase is unambiguously less ordered than the former. On the other hand, the molecules of lasalocid seem to stabilize the lipid membrane organization in the Lx phase as its characteristics are independent of the temperature up to the chain melting transition.

The low-angle X-ray diffraction patterns in the $0.005 \leq r \leq 0.04$ range, exhibit a phase transition around 40−41 °C which is accompanied by a decrease in the periodicity as for the $P_{\beta'} \leftrightarrow L_\alpha$ transition of pure DPPC (Figures 4A−F and 7A, B). The wide-angle diffraction patterns show a chain melting process for this transition. Above the transition, the lamellar reflections correspond to the existence of a single phase. At 45 °C, the repeat distance slightly increases from 66.4 Å for the L_α phase of DPPC to 69.5 Å for the Lx_α phase at $r = 0.04$ (Table 1, Figure 3B). The variation of 3 Å may result from an increase in the thickness of either the phospholipid bilayer or the water layer between the bilayers. The second hypothesis of a swelling induced by LAS seems to be ruled out because the variations of the bilayer repeat distances (lipid + water thickness) between 36 and 45 °C, i.e., below and above the chain melting transition, are very similar (6.1 and 5.3 Å, respectively, Table 1) for pure DPPC and the LAS/DPPC Lx phase. The increase observed in the periodicity could rather come from the localization of LAS molecules near the lipid polar headgroup−water interface. It might also be due to a lateral compression of the fluid chains by the ionophore acting as a yoke between the polar headgroups of the lipid. This action would result in stiffening of the bilayer. The rigidification of DPPC monolayers by LAS observed by surface pressure measurements[29] is in favor of this last hypothesis. It is worth noting that the insertion of the LAS molecules in the polar headgroups is independent of the structural arrangement of the hydrocarbon chains either in a gel or in a disordered state.

For $r = 0.05$ and $r = 0.06$, as long as the DPPC chains are in the gel state, a lamellar phase (Figure 8A) is still observed although the organization state of this phase is markedly less and less ordered than the Lx phase as the diffraction profiles are more and more broadened (Figure 3A). For $r = 0.08$, the repetition of the reflections no longer strictly corresponds to a lamellar organization (Figure 8A). This reflects that the structural arrangement of the DPPC bilayers becomes strongly perturbed by the insertion of LAS. The drastic increase in the long spacings (Table 1) and the evolution of the reflection profiles observed from $r = 0.05$ to 0.08 indicate a new type of interaction between the LAS and DPPC molecules. This suggests a change in the assembly of the ionophore molecules which could be gathered together to create, with a number of DPPC molecules, a new local structural organization forming distinct domains in the bilayer (see section below Insertion Mode of the Ionophore). The formation of this local organization leads to a linear increase in the bilayer thickness (lipid + water). Because the DPPC molecules may be estimated to be already fully extended and normal to the bilayer plane in the Lx phase, the increase observed in the periodicity should come from an increase in the interlamellar water layer thickness resulting from electrostatic repulsions created by the new organization of the LAS molecules. In the gel state, the local organization remains entrapped in the DPPC bilayers as the low-diffraction data indicate a monophasic domain. However, the structural disordering denoted by the broadening of the low-angle reflections can be interpreted as the existence of constraints due to the insertion of the LAS molecules which create defects in the planarity of the membrane. This leads to the existence of a "heterophase" which loses its lamellar character at $r = 0.08$.

In the $0.05 \leq r \leq 0.08$ range, with increasing the temperature up to 30 °C, the constant profile of the diffraction peaks (Figure 4G−I) indicates that the structural arrangement of the lipid membrane is not temperature-dependent. In contrast, between 30 °C and the temperature (37−38 °C) of the phase transition (Table 2), the diffraction peaks become clearly sharper as their intensities strongly increase. This reflects that at least part of the lipidic membrane adopts a structural arrangement more ordered than at 25 °C. This can be explained by considering that the lateral constraints imposed to the bilayer at 25 °C by the insertion of the aggregated LAS molecules are progressively weakened above 30 °C, leading to the recovery of a planar membrane surface.

In contrast, when the hydrocarbon chains are in the fluid state, two distinct species would coexist, as evidenced by the double reflections detected in the low-angle diffraction patterns, just above the phase transition (Figure 8). The observation of a decrease of the repeat distance for one of the double reflections (Figure 8A) during the phase transition process depicts a chain melting behavior similar to that observed for the $Lx \leftrightarrow Lx_\alpha$ phase transition at $r = 0.04$ (Figure 7B). This result suggests that, in this r range, the Lx_α phase still exists above the phase transition. It is worth noting that the poor resolution obtained for the second order prevents to define precisely the lamellar repetition. However, this phase would coexist with another species responsible for the reflections located at a lower q. A hypothesis could be that the new local structure formed by aggregated LAS molecules and which is embedded in the Lx phase at 25 °C could be transformed into isolated species above the phase transition as a consequence of the melted state of the DPPC acyl chains. As seen from the evolution of the relative intensities of both reflections versus r (Figure 8B), the proportion of the Lx_α phase would decrease to the benefit of the aggregated LAS containing structure. As this last organization is LAS rich, its repeat spacing increases as a function of LAS content (from about 74 to about 100 Å), while the periodicity of the Lx_α remains relatively constant (Figure 8A).

The absence of any lamellar reflection (Figure 9) observed for $r = 0.1$ and 0.12, whatever the temperature, suggests that the insertion of aggregated LAS molecules has transformed the lamellar arrangement of the DPPC bilayers into species the organization of which gives rise to diffuse bands in the RX patterns (Figures 4J, K and 9). The very broad bandwidths observed above and below the transition clearly resemble more and more the aggregate scattering patterns (Figure 9). The transition observed around 35−37 °C does not result into the band splitting observed for $0.05 \leq r \leq 0.08$. The diffraction line attributed from $r = 0.05$ to 0.08 to the fraction of the DPPC

membrane retaining the organization of the Lx_α phase is no longer detected. In parallel, the endotherm related to the $Lx \leftrightarrow Lx_\alpha$ transition is absent on the thermal recordings (Figure 10) [see section below on thermotropic behavior]. These results confirm the disappearance of a lamellar organization. It is worth noting that the DPPC molecules involved in the non lamellar structures still present a crystalline state between 25 and 35 °C since an interchain spacing centered at 4.2 Å is observed on the wide-angle diffraction patterns (Figure 1).

Sankaram et al.[28] have observed in the ^{31}P NMR spectra of DPPC multilamellar suspensions containing a high lasalocid content the appearance of an isotropic peak at 60 °C which agrees with the formation of aggregates. These authors have interpreted this result as being due to the formation of small lipid−ionophore aggregates. They compared these structures to the "reverse micellar aggregates" involved during membrane fusion or transbilayer transport processes. The evolution of the profile of the X-ray patterns obtained in the high concentration range of the ionophore may indicate the progressive formation of mixed aggregates (Figure 9). In this hypothesis, the DPPC bilayers would be progressively broken into smaller and smaller elements as it is not possible to insert more ionophore molecules without disrupting the lipid lamellar arrangement.

Thermotropic Behavior of the LAS/DPPC Multilayers. In the temperature range of the study, pure DPPC undergoes the well-known $L_{\beta'} \leftrightarrow P_{\beta'}$ pretransition and $P_{\beta'} \leftrightarrow L_\alpha$ main transition (Figure 7A). The disappearance of the pretransition in the thermal recordings above $r = 0.02$ (Table 2) is in agreement with the diffraction results. For $0 \leq r \leq 0.02$, the decrease in the transition temperature and the broadening of the pretransition peak confirm the existence of a two-phase domain. The decrease in the associated enthalpy (Table 2) may be explained as follows: the DPPC molecules which are under the influence of the LAS molecules no longer undergo the pretransition. These molecules are therefore subtracted from the transition, and the enthalpy measured is only relative to pure DPPC molecules which are still capable of exhibiting the ripple structure. This requires the existence of distinct domains in the DPPC membrane as evidenced by X-ray diffraction measurements.

Up to $r = 0.04$, the transition observed at 41 °C (Table 2) is characterized by a single thermal event (Figure 10). The evolution of the short spacing as a function of temperature (Figure 2) indicates that this thermal event corresponds to the melting of the hydrocarbon chain as for pure DPPC. Then in the hypothesis of the coexistence of the $P_{\beta'}$ phase of DPPC with the DPPC/LAS Lx phase, the endothermal peak depicts in a continuous way the melting of the DPPC hydrocarbon chains involved both in the $P_{\beta'}$ phase and in the Lx phase. As the DPPC chains are involved in both phases, the temperature of the transition and the enthalpy change (ΔH) expressed per mole of DPPC in the DPPC/LAS mixtures (Table 2) allow to compare the lipidic chain state in the Lx phase with respect to the chain organization in pure DPPC. The very slight decrease of the transition temperature observed (Table 2) and the ΔH remaining unchanged indicate that the structural arrangement of the lipidic chains in both phases should be very close. The main modification induced by the Lx phase lies in the broadening of the transition. Thus, the effect of LAS on the lipidic chain melting process essentially results in a significant decrease in the cooperativity of the transition. In the bilayers of pure DPPC, the disordering of one chain provokes that of the other molecules as a whole, rendering the melting process highly cooperative. LAS acts as a barrier in the lateral diffusion of the melting process which therefore is slowed. As the total number of DPPC molecules interacting with the ionophore increases, the cooperativity decreases and the broadening of the transition is amplified. In contrast, the constant value found for ΔH up to $r = 0.04$ (Table 2) means that all of the DPPC molecules in the DPPC/LAS mixtures take part in the transition. It results that the ionophore molecules are loosely bound to the DPPC molecules since the interaction does not change the ΔH of the transition.

From $r = 0.05$, the appearance of shoulders below and above the main thermal peak (Figure 10) corresponds to the formation of the new structural species observed above the transition in the low-angle diffraction patterns (Figure 8). Whereas the wide-angle patterns depict a lipid chain melting phenomenon as a whole (Figures 1 and 2), the profile of the thermal peaks reflects distinct DPPC chain states or at least a chain melting process occurring through several steps.

For $r = 0.05$ and 0.06, the main peak (Figure 10) is related to the transition ($Lx \leftrightarrow Lx_\alpha$) of the DPPC molecules which globally maintain the lamellar organization of the Lx phase (Figure 7B) while the DPPC molecules associated with the aggregated lasalocid molecules undertake separate chain melting transitions. Despite the existence of overlapped peaks, the ΔH of the whole transition does not decrease compared to $r = 0.04$. This indicates that the proportion of the Lx phase in the LAS/DPPC mixtures diminishes with increasing r. This behavior depicts a lateral phase separation within the lipid bilayers. The molecular arrangement of the lipids is markedly influenced by the presence of the aggregated ionophore. For the ratios 0.1 and 0.12, although the lamellar organization of the lipid membrane is no longer observed, the existence of two successive thermal transitions, in addition to the wide-angle patterns (Figure 1), indicates a persistence of an organized state of the DPPC molecules.

Insertion Mode of the Ionophore. Many antibiotic molecules such as LAS display a lateral distribution of the polar/apolar characters all along the molecule axis which delimits a hydrophilic part opposite to a hydrophobic one. This molecular geometry contrasts with that of most long-chain amphiphiles (e.g., phospholipids and surfactants) for which the distribution is longitudinal rather than transversal. These distinct geometries determine the specific behavior of these two classes of molecules.

At low antibiotic concentration ($r \leq 0.04$), X-ray diffraction and calorimetric results indicate that the lasalocid molecules do not present direct interaction with the acyl chains of the DPPC bilayers. This is in favor of a localization of the ionophore in the headgroups of the lipid at the water interface. The ionophore may be inserted in its extended conformation between the lipid polar groups with the polar part of the ionophore molecule interacting with the polar groups of the lipid and the hydrophobic part of the ionophore being oriented toward the lipid chain without interacting with them. The polar environment at the water interface is favorable to an extended conformation of the antibiotic.[2,15] Binding of the antibiotic to phospholipid headgroups has been evidenced by fluorescence studies[7,16,26,27] and circular dichroism experiments.[9] ^{31}P NMR studies on the insertion of lasalocid in multilamellar suspensions of DPPC[28] have shown that the lasalocid molecules were intercalated between neighboring headgroups, resulting in removal of headgroup phosphate−choline interactions.

Chong et al.[60,61] have proposed a model for the lateral organization of sterols in lipid membranes. When guest molecules are introduced in lipid bilayers, these molecules can either be randomly distributed, regularly distributed, or segregated in

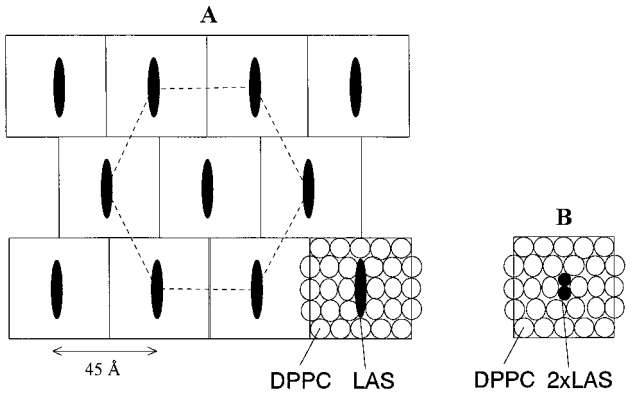

Figure 11. Schematic representation of the insertion of the antibiotic in DPPC bilayers: (A) insertion parallel to the membrane surface, hexagonal superlattice at $r = 0.04$; (B) insertion perpendicular to the membrane surface at $r = 0.08$.

separate domains. The lateral distribution depends on different parameters: the mixing ratio, temperature, pressure, and the intermolecular energies. In the low antibiotic concentration range ($r \leq 0.04$), the ionophore molecules may be either randomly or regularly distributed within the polar headgroups of the DPPC membrane. On the basis of the model proposed by Chong,[60,61] a regular lateral distribution of the ionophore in the membrane requires that (i) the interaction between lasalocid and DPPC molecules be stronger than the interaction between the DPPC molecules or the ionophore molecules themselves and (ii) the lasalocid molecules must be maximally distant from each other into a well-defined regular pattern in the plane of the DPPC membrane.

Upon addition of the antibiotic, the disappearance of the interactions between the polar headgroups of DPPC observed by ^{31}P NMR[28] indicates that the interactions between the antibiotic and the lipid molecules prevail over those between DPPC molecules. In addition, the lasalocid molecules can be inserted as monomers in the lipidic membrane as inferred by the linear increase in the fluorescence intensity observed upon addition of the antibiotic in the phospholipid membrane at low antibiotic concentration.[26,30] The existence of a unique lamellar structure at $r = 0.04$ (i.e., one LAS per 25 DPPC molecules) is consistent with a homogeneous antibiotic and lipid distribution. Therefore, the organization of the LAS molecules in the Lx phase can be interpreted in terms of a hexagonal superlattice model.[60] In the Lx phase, the acyl chains of the DPPC molecules adopt a hexagonal arrangement as shown by the wide-angle X-ray data. The low compactness of this hexagonal lattice[62] may favor the repartition of the LAS molecules. Assuming the ionophore molecules in the DPPC polar groups are maximally separated, they form a hexagonal superlattice. Such a molecular distribution is illustrated in Figure 11A. This defines regular areas in the plane of the bilayers so that the DPPC molecules are ordered by the lasalocid molecules. This ordering may also explain the stabilizing effect of the ionophore molecules on the conformational organization of the acyl chains in the Lx phase that is insensitive to the temperature up to 40 °C (Figure 7B, C).

The thermal behavior of the LAS/DPPC mixtures is suddenly modified from $r = 0.05$ (Figure 10). The appearance of shoulders below and above the main transition peak reflects interaction of lasalocid molecules with the DPPC acyl chains, indicating that, from this antibiotic/lipid ratio, the ionophore is capable of penetrating inside the hydrophobic interior of the lipid bilayers. This is rendered possible through dimeric structure of the ionophore. The ionophore molecules may be gathered with hydrophilic sides together in order to expose their hydrophobic moiety to the lipid hydrocarbon chains. In a linear conformation with all of the oxygen atoms on one side and all of the hydrophobic groups on the other side, the length of the ionophore (about 25 Å) approximates the length of a phospholipid hydrocarbon chain.[23] This is in agreement with insertion of LAS within the thickness of a monolayer.[31,32] The aggregated LAS molecules could therefore be inserted perpendicular to the membrane surface with one dimeric structure in each monolayer (Figure 11B). Conformational studies have shown that the ionophore exists as a monomer in polar solvents[63] and aggregates into a dimer in nonpolar solvents.[3] Thus, insertion of the ionophore inside the bilayer through dimeric structures would result from the conformation of the antibiotic molecules in a nonpolar medium. Although lasalocid dimers have been detected in organic solvents, the possibility of higher order aggregates in the membrane cannot be ruled out.

Ionophore self-association in lipid membranes at high antibiotic concentrations is also supported by fluorescence quenching resulting from intermolecular interactions between fluorescent groups (salicylic group) occurring during formation of an aggregate.[7,26,30] Quenching of the fluorescence intensity has been observed above an ionophore/lipid molar ratio of 1:22. This critical ratio is very close to the composition of the Lx phase. Thus, change in the mode of implantation occurs from a specific antibiotic/lipid molar ratio. Aggregation of lasalocid molecules above $r = 0.04$ leads to the formation of segregated domains in the bilayers as inferred from XRDT and DSC results.

Such a double mode of implantation has also been observed with alamethicin, an amphiphilic helix-forming peptide,[64] although the implications of both modes of insertion on the structural features of the lipid membrane are quite different for these two types of antibiotics.

Phase Diagram of the LAS/DPPC System. A schematic phase diagram in the LAS/DPPC ratio range studied can be deduced from the thermotropic and structural data discussed above. Figure 12 illustrates the different phase domains and their boundary limits as a function of temperature and LAS/DPPC ratios. The transition temperatures are obtained first from the enthalpimetric measurements but also from the structural features of the bilayer periodicity. The chain melting temperature is also clearly evidenced from the evolution of the interchain spacings as a function of the temperature.

The low-angle diffraction data show that the lamellar Lx phase is created as soon as the first LAS molecules are introduced into the DPPC multilayers. Its coexistence domain with the $L_{\beta'}$ and $P_{\beta'}$ phase of pure DPPC can be located between $r = 0$ and 0.04, for which the ripple structure completely vanishes. The existence of the Lx phase as a single one is centered around $r = 0.04$, as traces of the ripple structure are still detected at $r = 0.03$ and modifications in the low-angle diffraction patterns and the thermal recordings are clearly observed for $r \geq 0.05$. The composition of the Lx phase, which corresponds to 1 mol of LAS per 25 mol of DPPC, would represent the upper limit of insertion of the ionophore molecules as monomers in the DPPC bilayers with a regular distribution into a hexagonal superlattice according to the model proposed above. In the gel phase between $r = 0.05$ and $r = 0.08$, the formation of local structures in the lamellar organization of the Lx phase is indicative of a tendency to create a two-phase domain although these structures do not give rise to separate reflections on the X-ray patterns in the experimental conditions used. There is a continuous passage from the Lx phase to a local new structure in the bilayer. Indeed, each LAS molecule

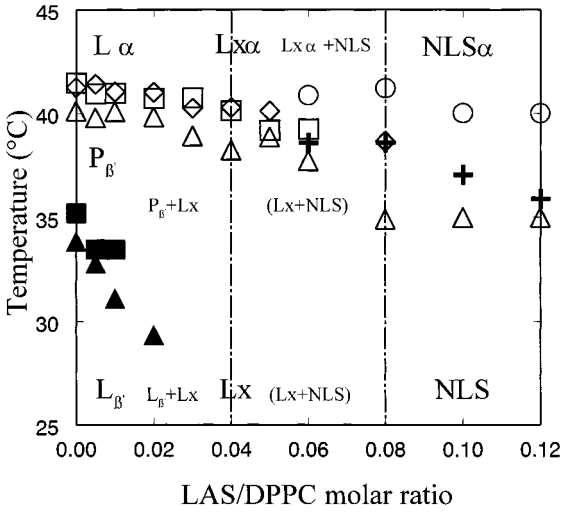

Figure 12. Schematic phase diagram of the LAS/DPPC/water system. The transition temperatures determined both from DSC and XRDT measurements have been plotted as a function of LAS/DPPC molar ratio: DSC (■) pre- and (□, +, ○) main transition temperatures; XRDT temperatures deduced from the long spacings of the (▲) pre- and (△) main transitions and from the short spacings of the (◇) main transition. The existence domain of the different phases is delimited from X-ray data. For the nomenclature of the phases see text. NLS refers to nonlamellar structure. The "pseudo-binary" phase diagram presented corresponds to a vertical cut of the ternary LAS/DPPC/water phase diagram being plotted versus temperature on a vertical axis. The *x* scale is expressed as LAS/DPPC ratio rather than mol % for coherence with the above results. The vertical dashed lines indicate the position of the phases corresponding to the schematic representation of Figure 11.

added to the Lx phase above $r = 0.04$ changes the orientation of one LAS molecule previously extended parallel to the membrane surface in the DPPC polar headgroups, both LAS molecules forming then a dimeric structure which inserts normal to the lipid surface in each DPPC monolayer (Figure 11). At $r = 0.08$, all of the LAS molecules are oriented perpendicularly to the membrane surface. The shoulders observed from $r = 0.05$ above and below the thermal peak attributed to the chain melting transition of the Lx phase (Figure 10) could reflect two organizational states for the acyl chains in interaction with the dimeric LAS aggregates. A number of DPPC molecules are strongly disordered and present a melting transition at a temperature lower than that of the Lx phase, whereas those interacting more tightly with the ionophore display a higher melting transition. Above $r \geq 0.08$, only nonlamellar species which could be membrane fragments seem to exist. The disappearance of a lamellar structure at a ratio corresponding to twice the ratio $r = 0.04$ is consistent with the formation of dimeric ionophore structures.

When the DPPC hydrocarbon chains are in a fluid state, a monophasic domain is observed up to $r = 0.04$. This is not surprising because the acyl chain arrangement is quite similar in the DPPC $P_{\beta'}$ and Lx phases and the DPPC L_α phase recovers a planar polar group surface. In the 0.05−0.08 ratio range, the lipid domains forming the heterophase in the solid state give rise to the coexistence of two separate phases (Lx_α and nonlamellar species) as inferred by the low-angle diffraction observations. Above $r = 0.08$, only nonlamellar species are observed.

Conclusion

XRDT and DSC measurements exclusively reveal the changes of the molecular arrangement of the DPPC multilayers caused by introduction of LAS at various concentrations. Interestingly, the results of this study are in agreement with the observations obtained by fluorescence measurements which come from the fluorophore of the antibiotic molecules and not from the lipid membrane.

Correlation of results obtained by DSC analysis and X-ray diffraction as a function of temperature at both wide- and low-angles provides important information at different levels: the distribution of the antibiotic molecules in the membrane matrix, its localization in the hydrophilic or hydrophobic part of the lipid membrane, the way of the antibiotic implantation depending on its concentration, the formation of local structures which may give rise to the existence of two-phase domains within the membrane. The whole body of data allow to construct a schematic phase diagram as a function of the temperature and the antibiotic/lipid molar ratio. This diagram gives a description of the lateral organization of the mixed antibiotic/DPPC bilayers and the stoichiometry of the different structures encountered as a function of temperature and antibiotic concentration.

Our results indicate that, even at very low concentration, lasalocid disorganizes DPPC in the gel state, while in the fluid state, the lipid phase is not affected by the antibiotic up to $r = 0.04$. However, above this ratio the progressive disappearance of a lamellar organization which is complete for $r = 0.08$ in both the gel and fluid state reflects the strong destructive effect of lasalocid on the lipidic membrane. The behavior of LAS in the fluid state of DPPC above the phase transition provides information about the perturbations that the ionophore may induce in biological membranes. It results that local accumulation of the antibiotic in cell membranes may have implications on the physiological effects that the ionophore can initiate.

Acknowledgment. The authors gratefully thank C. Betrencourt (G.R.P.B., Université René Descartes-Paris V, France) for her helpful contribution in sample preparation, C. Bourgaux for careful tune-up of the station D-24 of the DCI synchrotron (L.U.R.E., Orsay, France), and G. Keller for the elaboration of the XRDT sample holder.

References and Notes

(1) Bycroft, B. W. *Dictionary of antibiotics and related substances*; Chapman and Hall: London, 1988; p xv.
(2) Painter, G. R.; Pressman, B. C. *Top Curr. Chem.* **1982**, *101*, 83.
(3) Pressman, B. C. *Annu. Rev. Biochem.* **1976**, *45*, 501.
(4) Johnson, S. M.; Herrin, J.; Lin, S. J.; Paul, I. C. *Chem. Commun.* **1970**, 72.
(5) Maier, C.; Paul, I. C. *Chem. Commun.* **1971**, 181.
(6) Schmidt, P. G.; Wang, A. H.; Paul, I. C. *J. Am. Chem. Soc.* **1974**, *96*, 6189.
(7) Haynes, D. H.; Pressman, B. C. *J. Membr. Biol.* **1974**, *16*, 195.
(8) Degani, H.; Friedman, H. L. *Biochemistry* **1974**, *13*, 5022.
(9) Painter, G. R.; Pressman, B. C. *Biochem. Biophys. Res. Commun.* **1980**, *97*, 1268.
(10) Hasmonay, H.; Hochapfel, A.; Hadj-Sahraoui, A.; Jaffrain, M.; Peretti, P. *Thin Solid Films* **1992**, *210/211*, 747.
(11) Caswell, A. H.; Pressman B. C. *Biochem. Biophys. Res. Commun.* **1972**, *49*, 292.
(12) Kinsel, J. F.; Melik, E. I.; Lindenbaum, S.; Sternson, L. A.; Ovchinnikov, Y. A. *Biochim. Biophys. Acta* **1982**, *684*, 233.
(13) Degani, H.; Friedman, H. L. *Biochemistry* **1975**, *17*, 3755.
(14) Patel, D.; Shen, C. *Proc. Natl. Acad. Sci. U.S.A.* **1976**, *73*, 1786.
(15) Painter, G. R.; Pollack, R.; Pressman, B. C. *Biochemistry* **1982**, *21*, 5613.
(16) Haynes, D. H.; Chiu, V. C.; Watson, B. *Arch. Biochem. Biophys.* **1980**, *203*, 73.
(17) Pointud, Y.; Juillard, J. *J. Chem. Soc., Faraday Trans. 1* **1988**, *84*, 959.
(18) Lyazghi, R.; Hebrandt, M.; Tissier, M.; Pointud, Y.; Juillard, J. *J. Chem. Soc., Faraday Trans.* **1992**, *88*, 1009.
(19) Fernandez, M. S.; Celis, H.; Montal, M. *Biochim. Biophys. Acta* **1973**, *323*, 600.

(20) Hunt, G. R. *FEBS Lett.* **1975**, *58*, 194.
(21) Degani, H. *Biochim. Biophys. Acta* **1978**, *508*, 364.
(22) Degani, H.; Simon S.; Laughlin, A. C. *Biochim. Biophys. Acta* **1981**, *646*, 320.
(23) Chen, S.; Springer, C. S. *Biophys. Chem.* **1981**, *14*, 375.
(24) Shastri, B. P.; Sankaram, M. B.; Easwaran, K. R. *Biochemistry* **1987**, *26*, 4925.
(25) Cader, B. M.; Horrocks, W. de W. *Biophys. Chem.* **1989**, *33*, 265.
(26) Aranda, F. J.; Gomez-Fernandez, J. C. *Biochim. Biophys. Acta* **1986**, *860*, 125.
(27) Grunwald, R.; Painter G. R. *Biochim. Biophys. Acta* **1990**, *1027*, 245.
(28) Sankaram, M. B.; Shastri, B. P.; Easwaram, K. R. *Biochemistry* **1987**, *26*, 4936.
(29) Betrencourt, C.; Hochapfel, A.; Hasmonay, H.; Peretti, P.; Ollivon, M.; Grabielle-Madelmont, C. *Mol. Cryst. Liq. Cryst.* **1995**, *262*, 179.
(30) Chattopadhyay, A.; Komath, S. S.; Raman, B. *Biochim. Biophys. Acta* **1992**, *1104*, 147.
(31) Hasmonay, H.; Hochapfel, A.; Betrencourt, C.; Tahir, A.; Peretti, P. *Biochim. Biophys. Acta* **1994**, *1193*, 287.
(32) Hochapfel, A.; Hasmonay, H.; Peretti, P. *Mol. Cryst. Liq. Cryst.* **1995**, *270*, 23.
(33) Hochapfel, A.; Hasmonay, H.; Jaffrain, M.; Peretti, P. *Mol. Cryst. Liq. Cryst.* **1992**, *215*, 221.
(34) Keller, G.; Lavigne, F.; Loisel, C.; Ollivon, M.; Bourgaux, C. *J. Therm. Anal.* **1996**, *47*, 1545.
(35) Dahim, M. Ph.D. Thesis 1995, University Paris-Sud, France.
(36) Lavigne, F.; Bourgaux, C.; M. Ollivon *J. de Physique IV* **1993**, *3*, 137.
(37) Grabielle-Madelmont, C.; Perron R. *J. Colloid Interface Sci.* **1983**, *95*, 71.
(38) Janiak, M. J.; Small, D. M.; Shipley G. G. *Biochemistry* **1976**, *15*, 4575.
(39) M. J.; Shipley, G. G. *Biochim. Biophys. Acta* **1982**, *684*, 59.
(40) Wiener, M. C.; Suter R. M.; Nagle, J. F. *Biophys. J.* **1989**, *55*, 315.
(41) Luzzati, V.; Tardieu, A. *Annu. Rev. Phys. Chem.* **1974**, *25*, 79.
(42) Stamatoff, J. B.; Feuer, H. J.; Guggenheim, G.; Tellez, G.; Yamane, T. *Biophys. J.* **1982**, *38*, 217.
(43) Chapman, D.; Williams, R. M.; Ladbrooke, B. D. *Chem. Phys. Lipids* **1967**, *1*, 445.
(44) Hinz, H.-J.; Sturtevant, J. M. *J. Biol. Chem.* **1972**, *247*, 6071.
(45) Albon, N.; Sturtevant, J. M. *Proc. Natl. Acad. Sci. U.S.A.* **1978**, *75*, 2258.
(46) Marsh, D. In *CRC Handbook of Lipid Bilayers*; CRC Press: Boston, 1990; section II, p 139.
(47) Tardieu, A.; Luzzati, V.; Reman, F. C. *J. Mol. Biol.* **1973**, *75*, 711.
(48) Füldner, H. H. *Biochemistry* **1981**, *20*, 5705.
(49) Ruocco, M. J.; Shipley G. G. *Biochim. Biophys. Acta* **1982**, *691*, 309.
(50) Inoko, Y.; Mitsui, T. *J. Phys. Soc. Jpn.* **1978**, *44*, 1918.
(51) Lis, J. J.; McAlister, M.; Fuller, N.; Rand, R. P.; Parsegian, V. A. *Biophys. J.* **1982**, *37*, 657.
(52) Church S. E.; Griffiths, D. J.; Lewis, R. N.; McElhaney, R. N.; Wickman, H. H. *Biophys. J.* **1986**, *49*, 597.
(53) Nagle, J. N.; Zhang, R.; Tristam-Nagle S.; Sun, W.; Petrache, H. I.; Suter, R. M. *Biophys. J.* **1996**, *70*, 1419.
(54) Sun, W.-J.; Tristram-Nagle, S.; Suter R. M.; Nagle, J. F. *Biophys. J.* **1996**, *71*, 885.
(55) Ranck, J. L.; Mateu, L. M.; Sadler, D.; Tardieu, A.; Gulik-Krzywicki, T.; Luzzati, V. *J. Mol. Biol.* **1974**, *85*, 249.
(56) McIntosh, T. J. *Biophys. J.* **1980**, *29*, 237.
(57) Rand, M. J.; Chapman, D.; Larsson, K. *Biophys. J.* **1975**, *15*, 1117.
(58) Wittebort, R. J.; Schmidt, C. F.; Griffin, R. G. *Biochemistry* **1981**, *20*, 4223.
(59) Boroske, E.; Trahms, L. *Biophys. J.* **1983**, *42*, 275.
(60) Chong, P. L-G. *Proc. Natl. Acad. Sci. U.S.A.* **1994**, *91*, 10069.
(61) Chong, P. L-G.; Liu, F.; Wang, M. M.; Truong, K.; Sugar, I. P.; Brown, R. E. *J. Fluoresc.* **1996**, *6*, 221.
(62) Small, D. M. In *The Physical Chemistry of Lipids. Handbook of Lipid Research*; Plenum Press: New York and London, 1986; p 31.
(63) Chen, S.; Patel, D. J. *Proc. Natl. Acad. Sci. U.S.A.* **1976**, *73*, 4277.
(64) Wu, Y.; He, K.; Ludtke S. J.; Huang H. W. *Biophys. J.* **1995**, 2361.